I&EC research
Industrial & Engineering Chemistry Research

Article

Development of suitable CuO-based materials supported on Al2O3, MgAl2O4 and ZrO2 for Ca/Cu H2 production process

Laura Diez-Martin, Gemma Susana Grasa, Ramon Murillo, Andrew Scullard, and Gareth Williams

Ind. Eng. Chem. Res., **Just Accepted Manuscript** • DOI: 10.1021/acs.iecr.7b05103 • Publication Date (Web): 12 Feb 2018

ACS Publications

Industrial & Engineering Chemistry Research is published by the American Chemical Society. 1155 Sixteenth Street N.W., Washington, DC 20036

Development of suitable CuO-based materials supported on Al_2O_3, $MgAl_2O_4$ and ZrO_2 for Ca/Cu H_2 production process

Laura Díez-Martín[1*], Gemma Grasa[1], Ramón Murillo[1], Andrew Scullard[2], and Gareth Williams[2]

[1]Instituto de Carboquímica, ICB-CSIC, M Luesma Castan 4, 50018 Zaragoza, Spain

[2]Johnson Matthey Public Limited Company, London/United Kingdom

Corresponding author. Tel: +34 976733977; fax: +34 976733318

E-mail address: ldiezmartin@icb.csic.es

ABSTRACT

Functional materials for the sorption enhanced reforming process for H_2 production coupled to a Cu/CuO chemical loop have been synthesized. The performance of CuO-based materials supported on Al_2O_3, $MgAl_2O_4$ and ZrO_2 and synthesized by different routes has been analyzed. Highly stable materials supported on Al_2O_3 or $MgAl_2O_4$ synthesized by co-precipitation and mechanical mixing with sufficient Cu loads (around 65 %wt.) have been successfully developed. However, it has been found that co-precipitation under these conditions is not a suitable route for ZrO_2. Spray-drying and deposition precipitation did not provide the best chemical features to the materials. As the Ca/Cu process is operated in fixed bed reactors, the best candidates were pelletized and their stability was again assessed. Pellets with high chemical and mechanical stability, high oxygen transport capacity and good mechanical properties have been finally obtained by co-precipitation. The good homogeneity that provides this route would allow an easy scaling up.

Keywords: H_2 production, CO_2 capture, Ca-Cu looping process, CuO-based materials

1. INTRODUCTION

Hydrogen is an essential raw material used in chemical and refining industries for the manufacture of commodity chemicals like ammonia, methanol and fuels. H_2 can also be used as a clean source of energy to replace conventional fossil fuels in electricity generation. The demand of H_2 required from chemical and energy industries is increasing progressively [1]. On the other hand, greenhouse gases as CO_2, produced mainly in fossil fuel combustion, have increased their concentration in the atmosphere during the last decades and they are the main cause of the global warming. Therefore, it is necessary to develop new CO_2 capture technologies to mitigate the CO_2 emissions from large scale power plants and industrial processes in order to fulfill strict forthcoming environmental regulations [1, 2].

Steam Methane Reforming (SMR) is the most widely used technology to produce H_2 at commercial scale, producing around 50 % of the H_2 worldwide [3, 4], but at the expense of significant CO_2 emissions (9,1 - 8,9 kg CO_2 per kg H_2). The modern H_2 production plant is a stepped process where the reforming reactor is followed by a High Temperature Shift (HTS) reactor to maximize CO conversion and H_2 production [5, 6]. Finally, a pressure swing adsorption (PSA) unit is also needed when H_2 purities higher than 95 %vol. [7, 8] are pursued. At this point, hydrogen production combined with CO_2 capture and permanent CO_2 storage is presented as one of the potential routes to decarbonize the energy and industrial sectors. Although there are well-established routes to capture CO_2 in a concentrated form suitable for geological storage, the development of new technologies that allows the CO_2 capture cost to be reduced is also needed. In this context, the sorption enhanced methane reforming (SER) is a novel process of H_2 production that combines a reforming catalyst with a CO_2 sorbent (usually CaO) aiming

at removing the CO_2 as soon as it is formed [9]. Eq. (1) expresses the global reaction for the SER process using CH_4 as fuel and CaO as CO_2 sorbent. According to Le Chatelier's principle, the presence of the CO_2 sorbent shifts the equilibrium to the right achieving practically complete methane and CO conversions which leads to a higher hydrogen yield at relatively mild conditions of pressure and temperature. In addition, the final reaction is slightly exothermic because it combines one very endothermic reaction (steam reforming) with two exothermic reactions (shift and carbonation reactions).

$$CH_4(g) + CaO(s) + 2H_2O(g) \rightarrow CaCO_3(s) + 4H_2(g) \qquad \Delta H_{298K} = -13.7 \text{ kJ mol}^{-1} \qquad (1)$$

$$CaCO_3(s) \rightarrow CaO(s) + CO_2(g) \qquad \Delta H_{298K} = +178.5 \text{ kJ mol}^{-1} \qquad (2)$$

Multicycle operation of SER process requires the continuous regeneration of the sorbent by calcining the $CaCO_3$, Eq. (2), into CaO and CO_2 . This is a highly endothermic reaction (ΔH_{298K}= 178.5 kJ mol^{-1}) and it has to be performed in a CO_2 rich environment if the process aims at capturing the CO_2. In this way, an additional energy input is needed to reach the calcination temperature imposed by the equilibrium [9]. Among different alternatives proposed in the literature to reduce the energy penalty due to the sorbent regeneration [10-15], a new process known as Ca/Cu looping process was proposed [16]. This process makes use of a Cu/CuO chemical loop to solve the endothermic $CaCO_3$ calcination and to generate a CO_2 concentrated stream suitable for further purification and storage. At the same time, the process produces pressurized H_2 from CH_4 by steam reforming in presence of a CaO-based sorbent [7, 9]. The key point of this new technology lies in the fact of using the exothermic reaction of CuO reduction with additional CH_4 or other fuel gas to supply the energy for $CaCO_3$ calcination. In this way, the gas stream

that leaves the calciner will be ideally comprised of CO_2 and H_2O which can be easily separated by condensation.

The basic Ca-Cu looping process consists of a sequence of three reaction steps (see Figure 1), which are adiabatically carried out in fixed-bed reactors operating in parallel. In the first stage (stage A), an enriched stream of H_2 is produced by the sorption enhanced reforming of methane in the presence of a reforming catalyst, a CaO-based sorbent and a copper-based solid (that acts as inert in this stage). This takes place at 600 ºC - 750 ºC, steam-to-carbon molar ratios between 2.5 and 5, and pressures between 10 bar and 35 bar in order to achieve high H_2 production yields with high CO_2 capture efficiencies [17]. In the next stage (stage B), the copper-based material is oxidized with diluted air at high pressure. A low oxygen concentration in the feed moderates the increase of temperature during the oxidation of Cu to CuO, thereby avoiding the decomposition of $CaCO_3$ by partial calcination [18]. In the following reaction stage (stage C), the calcination of the $CaCO_3$ formed during the SER is accomplished by means of the simultaneous reduction of CuO with a gaseous fuel at atmospheric pressure. A suitable $CuO/CaCO_3$ molar ratio in bed composition has to be selected to ensure that the heat released during CuO reduction is sufficient to completely decompose the $CaCO_3$ without any external energy supply [19-21].

A detailed conceptual design of the process based on literature data was carried out by Fernández et al. [9]. In this work, simple reaction models served to define a range of operation conditions for the process in terms of Cu/Ca ratios and suitable operation pressures and temperatures for the different process stages.

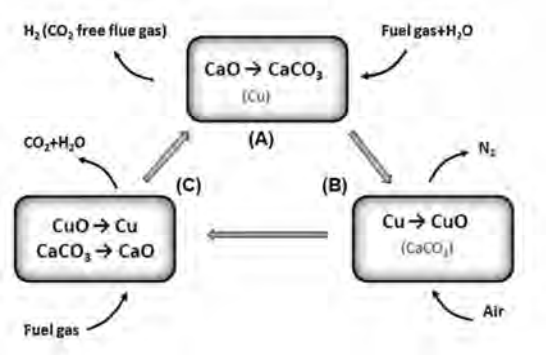

Figure 1. *General scheme of the novel Ca/Cu reforming process.*

A general layout of a complete H_2 production plant based on this process was designed by Martínez et al. [21] and promising results in terms of H_2 equivalent efficiencies were predicted by the model. Recently, experimental results in a pseudo-adiabatic fixed bed reactor were reported and confirmed the feasibility of supporting the calcination reaction of $CaCO_3$ with the exothermic reduction of CuO with H_2 [22]. Moreover, a relevant number of papers have been published describing in detail the different stages of the process [23-28].

A key aspect for the future development of the process is to have materials with optimum properties for cyclic operation [21]. With respect to the reforming catalyst, in principle, a commercial Ni-based catalyst has been proposed in the works by Fernández et al. [9, 23, 24] although more active materials currently under development could also be considered. The ratio Cu/Ca in the process will be determined by the requirements in the calcination step [7], and in order to reduce the thermal ballast of the inert fractions comprising the materials, it is necessary to maximize the active phase content of both the CaO based and the Cu-based materials [7, 9]. Some recent works are oriented to the development of composite materials containing CaO and CuO [29-34] and/or CaO and Ni acting as reforming catalyst [35-39]. With respect to the CaO-CuO composites, the results indicate that the progress of the carbonation reaction in the combined material might

affect negatively the kinetics of the oxidation reaction of Cu [31]. In addition, recent studies [30] produced mixed pellets with a Cu content around 50%wt. finding that the content of Cu/CuO has a significant influence on the cyclic performance of the CaO. The authors observed that the composites showed good reactivity for CuO but loss in CO_2 capture capacity after cycling. Moreover, the mechanical stability of the composite materials might be affected along cycling [34]. In general, these materials are still immature with respect to the use of individual pellets and important efforts on their development are required.

Focusing exclusively on CuO-based materials, a number of authors have published their results about CuO-based materials tested in Chemical Looping Combustion (CLC) [40-52], Chemical Looping with Oxygen Uncoupling (CLOU) [52-59], Chemical Looping Reforming (CLR) [60, 61] and Ca/Cu looping [22, 29, 34, 62] processes. Most of the work has focused on the development of oxygen carriers for CLC processes. The CLC technology has been confirmed by Lyngfelt et al. [63] that can be operated in a number of different units from 0.3 to 120 kW, with more than 4000 hours of operation using different oxygen carriers and wide variety of CuO-based oxygen carriers for CLC applications has been summarized in a review prepared by Adánez et al. [64]. The materials were prepared by different synthesis routes like freeze granulation, impregnation, extrusion, spray-drying, co-precipitation or mechanical mixing. The majority of the published works has referred to the use of Al_2O_3 as support [40, 41, 50, 53, 62, 65-69]. Several authors have recently developed high loaded CuO-based particles (around 70%wt. of Cu) by co-precipitation [50, 68] and they discovered that pH and the precipitating agent have a strong influence on the chemical structure of the materials [50]. They have tested their materials under 25 cycles and the results suggested that CuO reacted with Al_2O_3 to form fully reducible $CuAl_2O_4$ [49, 50]. Other promising results with materials onto Al_2O_3 has

obtained by Song et al. [51] that have reported a synthesis method based on layered double hidroxides (LDHs) precursors that improve the reactivity and stability of the materials achieving the homogeneous mix of the elements at molecular level. Mainly in order to avoid the formation of intermediates, other alternative support materials have been reported in the literature as $MgAl_2O_4$ [54, 65, 66], ZrO_2 [59, 65, 70], CeO_2 [52, 71] , TiO_2 [72], SiO_2 [60, 65] and combined metal oxides like $CuO\text{-}Fe_2O_3$ [73]. Regarding to the use of $MgAl_2O_4$ as support, Imtiaz et al. [58] has analyzed the effect of cycles on materials with Cu contents until 72%wt. and they found stable and close to the theoretical values for oxygen transport capacities during 25 cycles.

Since the Ca/Cu looping process is a relatively new concept, there are not many works published so far about Cu materials specifically designed and tested in fixed bed reactors. Most of the research has been developed in lab scale packed bed reactors using a mixture of CaO and existing commercial pellets of a Cu based material [22]. Although this work has shown promising results for the Ca/Cu looping process, additional efforts on the development of the pellets with high chemical and mechanical stability are still needed. In general, these new materials should have a high CuO load because the calcination enthalpy is considerably higher than the CuO reduction enthalpy. In agreement with the mass and energy balances of the process [9] materials with Cu loads between 55 to 70%wt. would be suitable candidates for the process. Therefore the development of highly stable CuO-based materials in pellet form that can be successfully adapted to reducing and oxidizing conditions, keeping oxygen transport capacity and mechanical strength during long number of cycles is an essential point in order to select the optimal CuO-based materials to achieve the highest energy yields during the calcination step of the Ca/Cu looping process.

Even though there are numerous studies about oxygen carriers for CLC or CLC-CLOU applications, there is still a need to evaluate how the synthesis route, the Cu load, and the particle or pellet form, might affect the performance of the materials under relevant conditions for Ca/Cu looping process. Therefore, the main objective of this paper is the development of stable CuO-based materials with suitable Cu contents for the Ca/Cu looping process. The effect that the inert support (Al_2O_3, $MgAl_2O_4$ and ZrO_2), the route of synthesis and the Cu load in the material has on the stability in terms of oxygen transport capacity (OTC) of the solids along oxidation/reduction cycles has been evaluated. The materials have been tested in powder and also pellet form, the latter being the final form in which the material will be introduced in the process [9]. The mechanical properties of the pellets after 150 cycles have been also evaluated.

2. EXPERIMENTAL

In this work, a wide range of CuO-based materials with Cu loads between 48.1 to 75.0 %wt., supported on Al_2O_3, $MgAl_2O_4$ and ZrO_2 and prepared by different synthesis routes, were analyzed. The range of Cu loads of materials has been selected in agreement with the mass and energy balances of the Ca/Cu looping process [9], that suggested that materials with Cu loads between 55 to 70%wt. would be suitable candidates for the process. The performance of the materials was evaluated in powder form (with up to 100 redox cycles in a TGA apparatus) and the most promising materials were also pelletized and tested in pellet form. The materials were texturally and physically characterized.

2.1. Description of the synthesis routes

Different synthesis routes were followed to prepare the Cu-based materials over Al_2O_3, $MgAl_2O_4$ and ZrO_2 as inert support. The materials that use Al_2O_3 as support were prepared by Johnson Matthey PLC (JM), while the rest of materials were prepared at the Instituto de Carboquímica (ICB-CSIC). Specifically, CuO-based materials were synthesized by spray-drying (JM), co-precipitation (JM and ICB), deposition-precipitation (JM) and mechanical mixing (JM). Figure 2 shows the steps followed in the synthesis routes evaluated in this research. All synthesis routes have common stages at the end of the process as for example drying and calcination steps. Specifically, regarding to the materials synthesized by ICB-CSIC via co-precipitation onto $MgAl_2O_4$ and ZrO_2, the calcination step during synthesis was carried out at 870 ºC during 2 hours using a heating rate of 50 ºC/min and the drying step was carried out at 120 ºC during 12 hours.

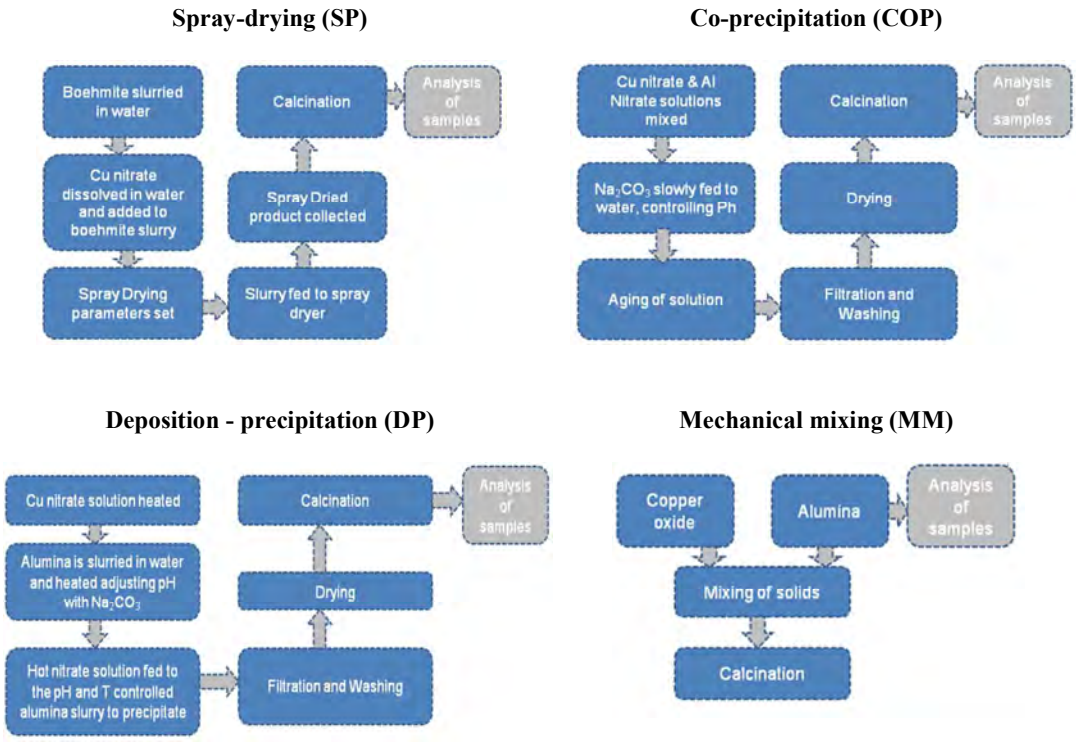

Figure 2. *Synthesis routes of CuO-based materials.*

Co-precipitation (COP): The CuO-based materials synthesized by co-precipitation were prepared following a specific co-precipitation method to achieve Cu contents between 48.1 to 75.0 %wt. Cu nitrate and Al or Mg or Zr nitrate solutions were mixed to synthesized the solids with a specific Cu load. Subsequently, the pH of the solutions was adjusted adding Na_2CO_3. The resulting mixture was stirred and filtered. During the filtration, the precipitate was washed several times with distilled water to remove excess nitrate and alkali ions. After that, the cake was dried and subsequently calcined in a muffle furnace. In the case of the materials synthesized by ICB-CSIC onto $MgAl_2O_4$ and ZrO_2, an specific amount of the Al and Mg or Zr nitrate solutions were mixed and shaken, adjusting the pH to 9,8 with Na_2CO_3 and calcining the sample at 870 ºC during 2 hours.

Spray-drying (SD): In the solids prepared via spray-drying, the copper nitrate solution was added to boehmite slurry. Then, the slurry was fed to a spray dryer and finally the material was also calcined in a muffle furnace.

Deposition - precipitation (DP): By this procedure, the copper nitrate solution was initially heated. In the same way, alumina was slurried in water and also heated adjusting the pH with Na_2CO_3. Secondly, the hot nitrate solution was fed to the pH and temperature controlled alumina slurry to obtain a precipitate. The precipitate was washed, filtered, dried and calcined.

Mechanical mixing (MM): This route consists of mixing copper oxide and alumina directly in a ball mill followed by the calcination of the sample.

Table 1 compiles a list of selected materials synthesized by SD, COP, DP and MM onto the different support materials. These materials were selected to be analyzed and characterized in detail among 25 materials initially tested in the TGA.

Moreover, some of the most promising materials were pelletized to test the mechanical stability in long periods of operation as the Ca/Cu reforming process requires.

Table 1: List and physical and chemical properties of selected CuO-based materials supported on Al_2O_3, $MgAl_2O_4$ and ZrO_2.

	CuO- based materials							Crystal size(nm)-Fresh samples		Crystal size(nm)-Cycled samples	
Reference	**Support-Synthesis**	**Cu** %wt.	**OTC exp.***	**OTC theor.**	**S_{BET}** m^2 g^{-1}	**ρ** kgm^{-3}	**ε (%)**	**CuO**	**$CuAl_2O_4$, $MgAl_2O_4$ or ZrO_2**	**CuO**	**$CuAl_2O_4$, $MgAl_2O_4$ or ZrO_2**
Cu75Al_SD	Al_2O_3-SD	75.0	0.187	0.189	6.2	5980		58.2	24.42	CuO: 27.47, Cu: 104.39, Cu_2O: 3.96, $CuAl_2O_4$: 12.24	
Cu65Al_COP	Al_2O_3-COP	65.5	0.164	0.164	20.5	5560	60	66.09	23.09	61.3	22.3
Cu63Al_DP	Al_2O_3-DP	63.0	0.157	0.159	17.3	5550		106.71	23.48	CuO: 27.53, Cu: 94.63, Cu_2O: 27.67, $CuAl_2O_4$: 14.51	
Cu60Al_MM	Al_2O_3-MM	60.4	0.151	0.151	21.4	5580		57.9	24.16	62.6	23.72
Cu70MgAl_COP	$MgAl_2O_4$-COP	69.0	0.174	0.176	12.1	5715		91.7	19.6	107.7	40.8
Cu65MgAl_COP	$MgAl_2O_4$-COP	65.0	0.163	0.163	20.9	5510	75	86.6	14.2	63.1	42.3
Cu60MgAl_COP	$MgAl_2O_4$-COP	59.7	0.151	0.151	13.7	6116		70.74	15.9	60.4	44.5
Cu72Zr_COP	ZrO_2-COP	72.4	0.08	0.181	5.1	6231		130.0	72.5	144.5	112.3
Cu67Zr_COP	ZrO_2-COP	67.3	0.144	0.169	4.1	6122		114.4	42.94	120.82	92.34
Cu48Zr_COP	ZrO_2-COP	48.1	0.111	0.121	1.7	6116		75.75	54.33	86.54	100.94

Methods of synthesis: SD (spray-drying), COP (co-precipitation), DP: (deposition -precipitation), MM (mechanical mixing).

**OTC exp.: average of the values collected up to 100 cycles. In the case of the material Cu72Zr_COP the values were collected until 25 cycles.*

It is important to highlight that in the case of two cycled samples (Cu75Al_SD and Cu63Al_DP) it has been found the presence of CuO, Cu, Cu_2O and $CuAl_2O_4$ as these samples could be partially reduced.

2.2. Characterization

The CuO-based fresh materials were analyzed by ICP-OES in order to determine their Cu content. The device used in these analysis was a Spectroblue apparatus of Ametek. All fresh and cycled samples were also characterized by X-ray diffraction (XRD) to identify crystalline species present in the solids and the average crystallite sizes before and after cycling. The device used for these analyses was an X-ray diffractometer Bruker AXS D8ADVANCE that employs CuKα radiation. The fresh materials were

characterized by TPR analysis to study the main temperatures of reducible species present in each CuO-based material. The analysis was carried out in a PulseChemisorb 700 supplied by Micromeritics. Specific surface area was calculated by N_2 physisorption applying the BET method in an Micromeritics ASAP 2020 apparatus and the solid density by He picnometry has been determined in a Micromeritics ACCUPYC II device. Also, some pictures of samples were taken after TGA cycling to show possible signs of agglomeration. Finally, the selected materials in powder and pellet form, were analyzed using SEM and EDX techniques to assess the dispersion of active phase and inert support. Scanning electron microscopy (SEM) coupled to energy dispersive X-ray (EDX) using a Hitachi S-3400 N were applied in order to determine the morphology and copper distribution in the samples. A Shimpo Dynamometer (FTS-20X) has been used to determine the horizontal crushing strength (HCS) of the selected pellets. This device measures the force needed to crush individual pellets, up to 100 N and the measurements served to calculate the average HCS value reported in the manuscript.

2.3. Apparatus

A thermogravimetric analyzer (TGA-CI Electronics Ltd.) was used to determine each material's chemical and mechanical stability under oxidizing and reducing conditions. This equipment consists of two concentrically-arranged quartz tubes located inside a furnace. Each sample was introduced in a platinum basket placed at the bottom of this device. Up to 100 oxidation/reduction cycles were performed on the materials in powder form (average particle size of 75μm) under isothermal conditions at 870 ºC. Around 15 mg of sample in powder form of each material were loaded in the platinum basket in every test. A constant total flow of 280 ml/min of gas was fed in at the top of

the reactor, after being preheated by flowing through the external reactor tube along the furnace with a space velocity of 0.012 m/s. Reaction temperature and gas composition were maintained constant in each test. Reduction and oxidation cycles were performed by a gas stream comprised of 20 vol% H_2 in N_2 and 20 vol% O_2 in N_2 respectively, using a N_2 purge between each reduction and oxidation stage. A constant N_2 flow passed through the head of the thermobalance to prevent any damage of the apparatus. The materials were collected after testing to be characterized. The Cu content in each material was calculated from the amount of oxygen reacting during successive reduction/oxidation cycles in the TGA. These values were later corroborated by the ICP data obtained in the laboratory.

The oxygen transfer capacity (OTC) and the active copper load of the materials were calculated from the data obtained in the TGA by the following formulas:

$$OTC = \left(\frac{m_{ox} - m_{red}}{m_{ox}}\right) \cdot 100 \quad (3)$$

$$x_{red} = \frac{m_{ox} - m(t)}{m_{ox} \cdot OTC} \quad (4)$$

$$x_{ox} = \frac{m(t) - m_{red}}{m_{ox} \cdot OTC} \quad (5)$$

Where m_{ox} is the weight of the material completely oxidized, m_{red} is the weight of the material completely reduced and m(t) is the instantaneous sample weight.

As it was mentioned before, some of the materials in powder form that presented the best chemical behavior were pelletized in order to analyze their chemical and mechanical stability in a long number of reaction cycles. Each pellet was tested using the TGA and approximately 150 reduction/oxidation cycles were done at 870 ºC following the same procedure that was applied with the materials in powder form.

3. RESULTS AND DISCUSSION

3.1. Characterization of oxygen carriers

Figure 3(a) shows the X-ray diffractograms of fresh and cycled samples of CuO-based materials synthesized by different routes and onto different supports. All the materials revealed that CuO is the more abundant species in the fresh material. It was also observed that a common feature of the materials supported on Al_2O_3 is the presence of $CuAl_2O_4$ in the crystalline structure. This compound was detected in all samples prepared by SD, COP and, DP. This species has been also detected by other authors that have been analyzed CuO-Al_2O_3 materials [66, 68, 74]. However, in this study the formation of $CuAl_2O_4$ was not observed in the materials prepared by mechanical mixing (MM). Hu et al. [74] studied the formation of copper aluminate spinel ($CuAl_2O_4$) and cuprous aluminate delaffosite ($CuAlO_2$) in copper-laden sludge that is thermally treated with γ-alumina and found four copper containing phases (CuO, Cu_2O, $CuAl_2O_4$ and $CuAlO_2$) in the investigated system. It was found that $CuAl_2O_4$ could be effectively formed between 850 ºC and 950 ºC by the γ-alumina precursor and $CuAlO_2$ is formed at higher temperatures (>1100 ºC) in the copper-alumina system. The XRD analysis carried out by Chuang et al. [67] with CuO-based materials prepared by mechanical mixing, wet-impregnation and co-precipitation revealed the presence of CuO and $CuAl_2O_4$ in fresh samples, but Al_2O_3 was not detected in any case. Although most of the initial Al_2O_3 could be forming $CuAl_2O_4$ in the samples, another possible explanation could be that Al_2O_3 was always present in its amorphous form and could not be detected by XRD [40, 58]. Imtiaz et al. [58] also observed only the presence of CuO and $CuAl_2O_4$ in CuO-Al_2O_3 solids prepared by co-precipitation. Therefore, it seems that the choice of a suitable route of synthesis of CuO based materials supported onto Al_2O_3, is a key aspect in order

to avoid the formation of copper aluminates. In this work, it has been confirmed that MM is a suitable method of preparation of this type of materials. Some of the ways in which $CuAl_2O_4$ can be formed from the decomposition of nitrate precursors occurs when aluminum nitrate forms amorphous alumina while heating or because the Cu and Al precursors are homogeneously mixed before heating [74]. In this way, the MM allows to use α-Al_2O_3 as a support material directly with CuO while using other type of synthesis routes the Al and Cu precursors would be practically homogeneously distributed in the sample and amorphous alumina could be formed that could react with CuO at much lower temperatures to form $CuAl_2O_4$. On the other hand, the presence of $CuAlO_2$, that could limit the amount of Cu that could be recovered as CuO in an oxidation cycle [69], has not been detected in any case. This means that fully CuO regeneration from $CuAl_2O_4$ is practically achieved in all cases. Therefore, the presence of $CuAl_2O_4$ in these samples is not a limiting step for the stability of the materials in agreement with results obtained by other authors [49, 50] that obtain stable reactivity for materials that also showed $CuAl_2O_4$ after synthesis.

In any case, for the CuO-Al_2O_3 prepared materials through SD, COP and DP, in this work, the ratio of intensity for the CuO and $CuAl_2O_4$ peaks is maintained for the cycled samples, indicating that the proportion of species is stable along cycling. In this way, in agreement with the thermodynamic study carried out by Jacob et al. [75] stable $CuAl_2O_4$ can be obtained at temperatures above 800 ºC.

In contrast with the CuO onto Al_2O_3 materials, no interaction was observed when $MgAl_2O_4$ was used as support. In agreement with results published in the literature [40, 53, 58, 73] these Cu-based materials were only comprised of CuO and the spinel $MgAl_2O_4$ according to XRD analysis. The presence of alumina or magnesia was not detected in the case of $MgAl_2O_4$ materials, indicating that all the Al_2O_3 and MgO formed the

$MgAl_2O_4$ or existed in amorphous phases. The $MgAl_2O_4$ spinel results in a very stable structure and no interference with CuO is observed.

In this way, it seems that the formation of the $CuAl_2O_4$ or $MgAl_2O_4$ spinels, respectively, using an appropriate calcination temperature after synthesis provides the material high stability and no interaction with the CuO active phase as stable cubic ordered structures for the spinels are formed in these conditions.

Regarding to the CuO-based materials with ZrO_2 as support, no formation of intermediate species was detected by XRD, as well as other authors that have been tested ZrO_2 materials [73]. However, we have discovered that the lattice parameters of the ZrO_2 phase found for these type of materials (a = 5.20 - 5.31 Å, b = 5.20 - 5.22 Å, c = 5.14 - 5.20 Å, β = 99º) correspond with the presence of monoclinic ZrO_2 (m-ZrO_2) in agreement with the values determined for this kind of chemical structure in the literature [76]. The structure m-ZrO_2 have been identified in all fresh and cycled samples of ZrO_2 solids, and this structure would not be suitable to obtain highly stable materials as it has been also reported by other authors [77, 78]. Therefore it seems that the modification of the ZrO_2 structure has a direct influence on the CuO reduction, and positive results have been found for catalysts in which the tetragonal surface of ZrO_2 (t-ZrO2) has been identified instead of the monoclinic (m-ZrO2) [78]. Several authors, have studied the tetragonal to monoclinic transformation [77, 79] and it seems that grain size, oxygen vacancies and compressive stress are important factors. CuO-ZrO_2 catalysts with tetragonal ZrO_2 were succesfully synthesized in the work published by Liu et al. [80]. Although their materials were prepared using a different method and lower Cu contents, the calcinations temperature during synthesis was rather low (450 ºC) than the temperature used in our solids (up to 800 ºC). Therefore, this elevated temperature could be related to the change from the tetragonal to the monoclinic phase of the ZrO_2.

Table 1 also compiles the crystallite sizes for the different materials before and after cycling as well as the specific surface area ($m^2\ g^{-1}$) and true density ($kg\ m^{-3}$). Regarding into the route of synthesis followed for the materials onto Al_2O_3, DP results in very high CuO crystals with respect to the other procedures that showed similar CuO crystals. On the other hand, materials with similar Cu loads (65%wt.) showed different size in CuO crystals depending on the support used. Then, the CuO crystal sizes were 66.1 nm for Al_2O_3, 86.6 nm for $MgAl_2O_4$ and 114.4 nm for materials onto ZrO_2. In addition, taking into account the materials with different Cu load prepared by the same route (COP) onto $MgAl_2O_4$ or ZrO_2, respectively, in general an increase on the CuO crystals is related with the increase in CuO content in the material. These results are in agreement with other works in which the growth of CuO crystals with the increase of Cu load has been also observed [81, 82]. Then, the growth of the CuO crystals could be related with the formation of bulk CuO, instead of highly dispersed Cu species [81] and the decrease in the strength of the $MgAl_2O_4$ or ZrO_2 lattice associated with this increase in the Cu load. Moreover, another aspect to remark for solids onto ZrO_2 by COP, is the high size of the ZrO_2 crystals (42.94 nm) related with monoclinic ZrO_2 with respect to the $MgAl_2O_4$ (14.2 nm) or Al_2O_3 (23.09 nm) crystals. Therefore the lowest ratios between the size of CuO and ZrO_2 crystals were found for ZrO_2 compounds that can be directly related with the monoclinic structure of ZrO_2, suggest clearly that the synthesis route for ZrO_2 solids must be modified. Moreover, taking into account the crystal sizes of the cycled samples of the CuO-ZrO_2 materials that are detailed in Table 1, it has been always observed an increase in the CuO and ZrO_2 crystals after cycling which could negatively affect the chemical stability of these materials.

Figure 3(b) shows the comparison between the results obtained from the TPR analysis for the materials onto the different supports. While the materials supported onto Al_2O_3

present two differentiated H_2 uptake peaks, the materials onto $MgAl_2O_4$ or ZrO_2 showed an only H_2 consumption peak. While pure CuO shows CuO reduction peaks around 350 ºC, in the case of the addition of supports to the CuO matrix, this value could be reduced [83].

All the materials shows a main H_2 consumption peak around 275 ºC and the total consumption of H_2 was very similar for the materials with the same Cu load into the different supports. However, in the case of the Al_2O_3 materials the two peaks are associated with the reduction of two different copper species. The main H_2 uptake peak is related to the reduction of a well-dispersed CuO, and the second minor peak at temperatures close to 400 ºC is attributed to the presence of $CuAl_2O_4$ in the materials.

Moreover, as it can be extracted from this figure, materials onto Al_2O_3 and ZrO_2 showed more defined peaks associated with CuO reduction than materials onto $MgAl_2O_4$ that presented wider peaks associated with this reaction. It seems that this aspect could be related with some kind of interaction between the CuO and the $MgAl_2O_4$ that facilitates the reduction of copper species in the material [84].

Comparing between synthesis routes, there are minor variations on the temperature at which the peaks present their maximum, although similar well-defined peaks for CuO were observed in the case of the materials prepared by COP as well as MM. It is also important to take into account that the solid synthesized by DP presents a non-defined peak for CuO formed by two little bends. This fact could be associated with the reduction of Cu(II) and Cu(I) species. Regarding to the peak at higher temperature, the MM materials presented the smallest peak, that indicates the presence of an small amount of $CuAl_2O_4$ undetected by XRD analysis. For the case of materials onto $MgAl_2O_4$ and ZrO_2, there is only one reduction peak in the range 250-350 ºC, that is wider for the materials onto $MgAl_2O_4$. On the other hand, the temperature associated

with the reduction of Cu^{2+} of the different CuO-based materials with similar Cu contents has varied slightly depending on the support. In this way, these temperatures have been determined as 220 - 230 ºC for materials onto Al_2O_3, 248 ºC for materials onto $MgAl_2O_4$ and 266 ºC for materials onto ZrO_2.

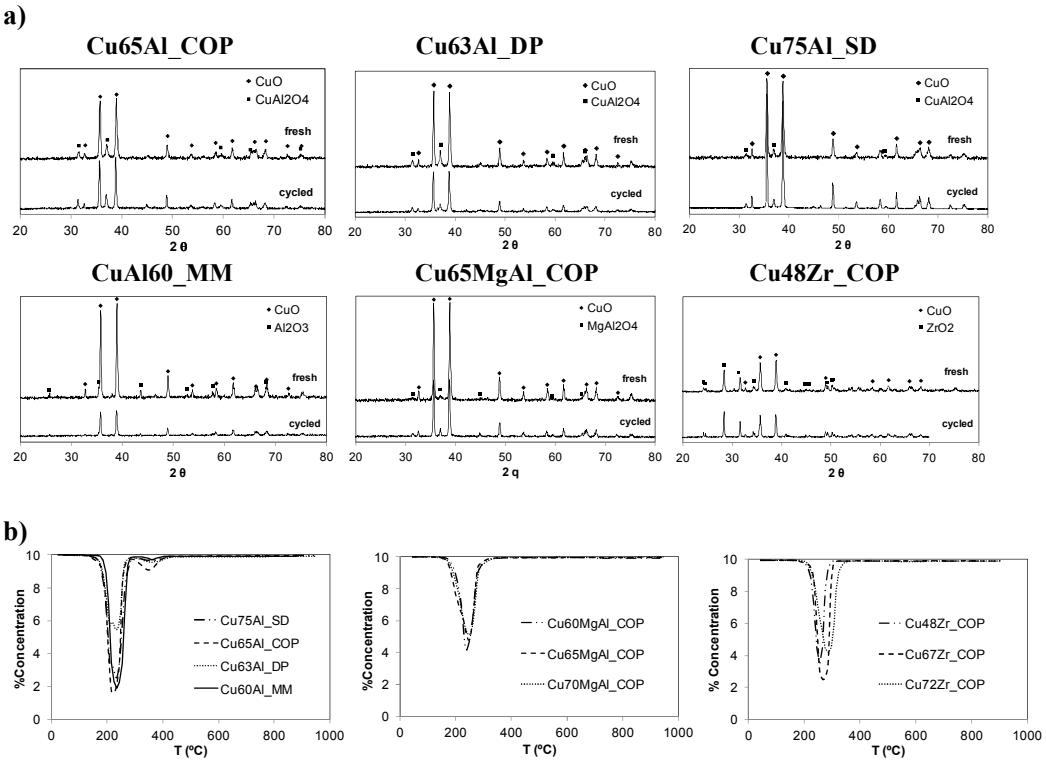

Figure 3: a) *XRD tests before and after TGA operation for solids synthesized by different techniques;* ***b)*** *TPR data for solids on different supports and prepared through different synthesis procedures: (left) Al_2O_3 as support, (center) $MgAl_2O_4$ as support and (right) ZrO_2 as support.*

Regarding to the BET surface area, Table 1 shows that the materials supported on $MgAl_2O_4$ or Al_2O_3 (synthesized by SD, COP, DP and MM) with Cu loads around 65%wt. presented similar values (close to 20 m^2 g^{-1}). However, the solids onto Al_2O_3 prepared by SD as well as the materials supported on ZrO_2 presented much lower

(below 7 $m^2 g^{-1}$) surface areas. In the case of the SD method, the low specific surface areas that show this kind of materials could be related with the absence of the strongly basic sites because no adjustment of the pH was carried out during the synthesis, and some authors have reported that the pH strongly influenced the structure of the oxygen carriers [50]. Other works in the literature have shown a progressive and important decrease in the values of the specific surface areas of CuO-ZrO_2 materials as the Cu load in the materials increased [85]. Águila et al. [81] showed that an increase in the Cu load favored the formation of large CuO particles, but the concentration of the dispersed copper species would remain constant which indicated a stabilization of the dispersed CuO species on some zirconia surface sites. Other published works showed an increase of specific surface areas for Cu loads up to 30 %wt. and a decrease in the BET surface area when the Cu content was over 50 %wt. [86]. The increase of surface area with an increase in Cu content was interpreted as being due to the contribution of the copper species to the tetragonal zirconia formation which indicates that the Cu is monodispersely distributed on the surface of ZrO_2. However, when the Cu content is greater than a certain value, copper could be incorporated in the zirconia lattice and amorphous composites could be obtained.

The porosity of the samples prepared by COP with similar Cu load (around 65%wt) has been determined and high values have been obtained for the Al_2O_3 (60%) and $MgAl_2O_4$ (75%) materials in powder form. Although the porosity of the pellets have decreased with respect to the materials in powder form (P_Cu65Al_COP_a = 48% and P_Cu65MgAl_COP = 43%), this values are considered suitable for this kind of materials. Finally, regarding to the CuO-samples density, the data obtained from He picnometry are in the expected range for these type of materials as it can be appreciated in Table 1 (5500 - 6200 kg m^{-3}).

3.2. Chemical and mechanical stability

3.2.1. Materials in powder form.

The chemical stability of the synthesized materials was evaluated in the TGA apparatus described in the experimental section. Approximately, 100 reduction/oxidation cycles were performed for each CuO-based material. The materials were tested according to the routines described in the experimental section. The theoretical OTC values and the experimental OTC values for each material at cycle 100 have been added to Table 1. Highly stable OTC values were obtained for the materials synthesized by COP onto Al_2O_3 and $MgAl_2O_4$ with 65%wt. of Cu load or below, but a dramatic decrease in the experimental OTC values was determined for the materials onto ZrO_2 with 72%wt. of Cu. In addition, Figure 4 shows the evolution of the OTC for materials with different Cu loads and onto the three supports tested in terms of the number of reaction cycles. According to this Figure, considering the materials with the highest Cu load for each support (over 70 %wt. Cu), the materials supported on Al_2O_3 and $MgAl_2O_4$ presented a fairly stable OTC and lost less than 5% of their initial transport capacity even after long periods of operation. In contrast a dramatic decrease in OTC nearly from the first cycle is well appreciated for the material supported on ZrO_2 and it is reduced by 60 % after 25 reaction cycles. Only the reduction of the Cu load below 50 %wt. resulted in stable materials for the system CuO-ZrO_2 since, as previously mentioned, limited by the formation of m-ZrO_2. The materials prepared by the different synthesis routes (DP, MM, COP) onto Al_2O_3 and $MgAl_2O_4$ with Cu contents around 65 %wt. and below, presented a highly stable oxygen transport capacity (losses below 1%).

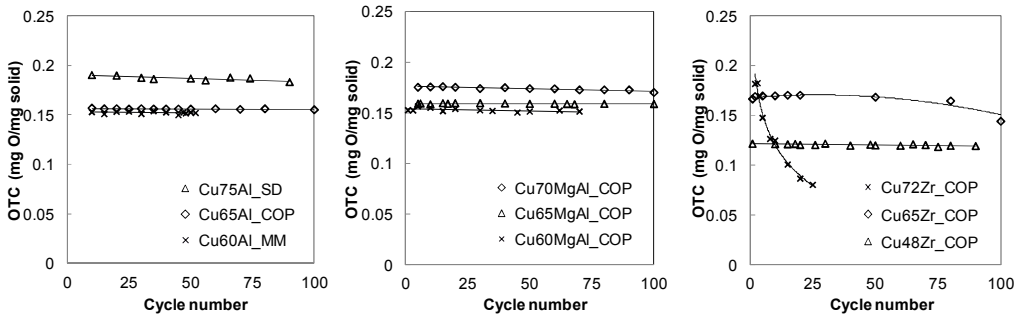

Figure 4. *Oxygen transport capacity (mg O transported/mg oxidized solid) in oxidation-reduction cycles: (left) CuO/Al_2O_3, (center) $CuO/MgAl_2O_4$ and (right) CuO/ZrO_2 material.*

With respect to the individual conversion curves on each cycle, Figure 5a shows examples of oxidation conversion curves for cycles 20 and 100 for materials with different Cu load and onto the different supports tested. With respect to the cycle 20, slight differences appear on the slope of the oxidation conversion curve among the materials supported onto Al_2O_3. A small second slope in the oxidation conversion was observed in all the materials except in the solid synthesized by COP. The differences in materials conversion curves at cycle 100 increased, and the oxidation curves for the materials synthesized by DP and MM, although were very similar along cycles, revealed that there could be other species in the materials due to the existence of a change in the slope of the Cu conversion curve for conversions higher than 0.9. This aspect is likely associated to the formation of small quantities of $CuAl_2O_4$ during the course of the oxidation reaction. Finally the SD material presented an important reduction on the oxidation reaction rate with cycles and the shape of the curve might indicate that diffusion phenomena might play a role during the oxidation of the material as the shape of the curve resembles the oxidation curves of the materials in which a collapse of the original chemical structure is produced. This is caused because the inert content in the material is not high enough to provide a high long-term chemical stability and mechanical stresses are caused between the active phase and the support. In the

past, some authors tested materials with 100%wt. of Cu load and they observed a dramatic decrease in the chemical stability with cycles [40]. Therefore, the morphological changes in the chemical structure of the materials with too high Cu loads after cycles, can cause a difficulty for the O2 to access to the Cu active sites and the diffusion of the gas can become important during the oxidation reaction.

In contrast, the COP material oxidation curve is almost unaltered with respect to cycle 20. Focusing on materials that use $MgAl_2O_4$ as support, materials with Cu contents up to 65 %wt. presented almost identical conversion curves at cycles 20 and 100, while the material with the highest Cu load (70 %wt.) presented a slight decrease in OTC. Also its oxidation conversion curve at cycle 100 presented an important decrease in reaction rate for conversions higher than 0.85. With respect to materials supported on ZrO_2, and in line with the data from Figure 4 for ZrO_2 materials, it can be observed that the material with the highest Cu load presented an oxidation conversion curve with a very slow reaction rate from the initial cycles, and as the number of reaction cycles proceeded only the material with Cu contents below 50 %wt. maintained the reactivity.

Figure 5b shows the reduction conversion curves of the different materials grouped by material support. During the first minute of these curves, a pure N_2 stream was feed to the TGA. A practically negligible loss in the weight of the samples is observed in this period which means that the CLOU effect is avoided under the operating conditions. After the first minute, a stream with 20 vol% of H_2 in N_2 was passed through the sample and very similar reduction conversion curves were obtained for all materials despite of its support or synthesis method, achieving total conversion in less than one minute. However, in the case of the materials onto Al_2O_3 prepared by SD, in agreement with the

results obtained on the oxidation reaction curves, the reduction reaction rate was a bit slower than for the materials onto Al_2O_3 prepared by other synthesis routes.

On view of the characterization results and the experimental data from Figure 4 and the experimental curves presented in Figure 5, it seems that the materials onto Al_2O_3 and $MgAl_2O_4$ with Cu contents between 60 to 65 %wt. could be suitable for the Ca/Cu process in terms of chemical stability. At this point the materials supported onto ZrO_2 were discarded from further study as the development of suitable CuO-based materials onto this support should be investigated at lower calcination temperatures during synthesis in order to obtain the structure t- ZrO_2. However the Ca/Cu looping process takes place at high temperatures and therefore the formation of m- ZrO_2 during operation would be also possible so the use of this support in this kind of processes should be avoided. Moreover, the Cu load that would allow for a stable material on ZrO_2 with the current m-ZrO_2 structure in the material would introduce an excessive inert fraction in the reactors which would affect negatively the process energy balances[9].

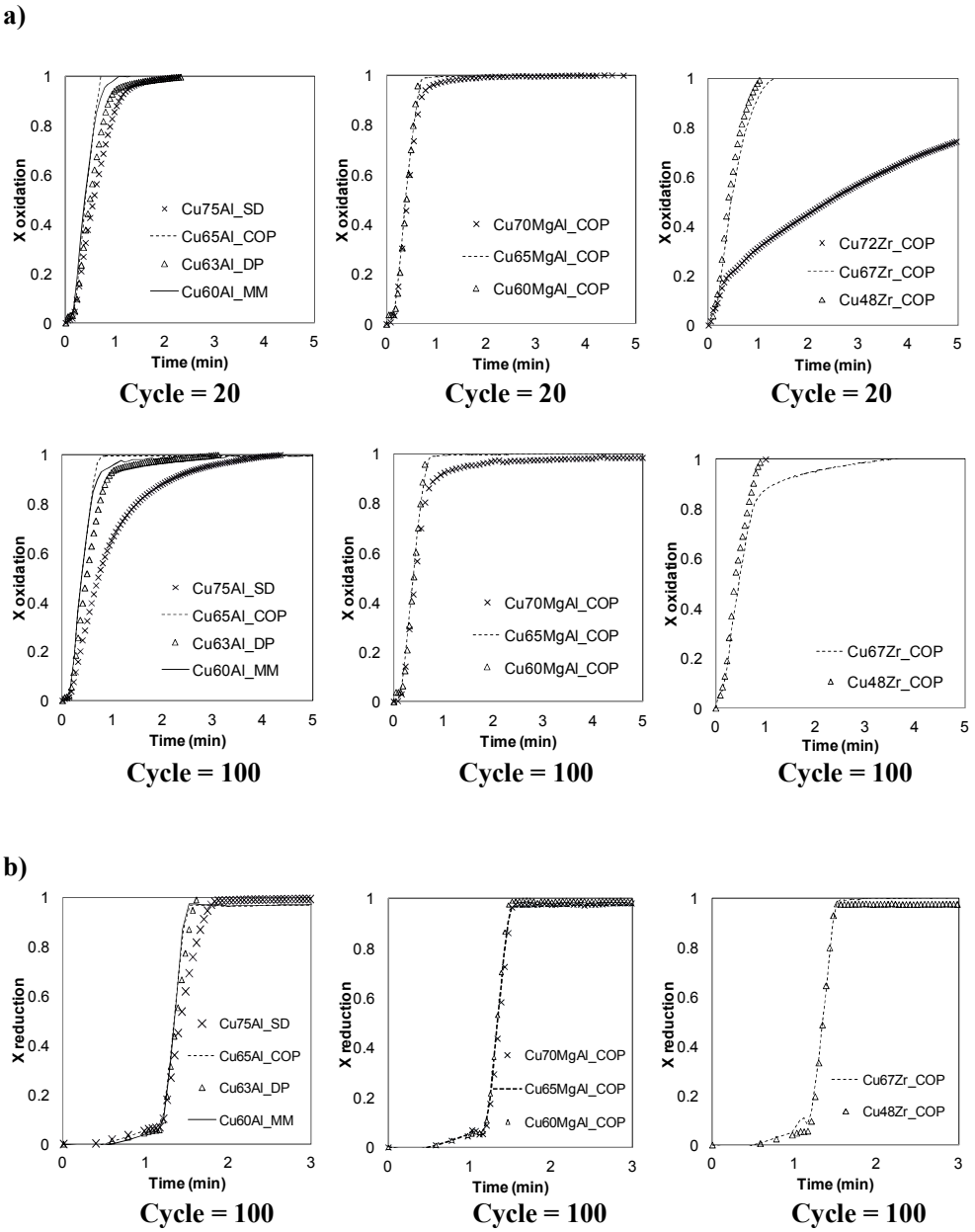

Figure 5: a) *Oxidation reaction curves of CuO-based materials depending on the material support (T=870ºC, 20vol% O_2, cycle number=20 and 100): (left) Al_2O_3, (center) $MgAl_2O_4$, (right) ZrO_2.* ***b)*** *Reduction reaction curves of CuO-based materials depending on the material support(T=870ºC, 20vol% H_2, cycle number=100): (left) Al_2O_3, (center) $MgAl_2O_4$, (right) ZrO_2.*

All the materials were examined after testing in the TGA to observe any sign of agglomeration caused by the redox cycles. In this way, the samples onto Al_2O_3 and

$MgAl_2O_4$ prepared by COP were not affected in any case by agglomeration phenomena. On the other hand, the samples synthesized by MM tended to form an external hard layer that was breakable but in contrast, high agglomeration was observed in SD and DP samples after the reduction/oxidation cycles.

In view of the experimental results obtained at this point, COP has been selected as a suitable route to produce materials with the best long term performance. Thereby, the materials with Cu loads around 65%wt. either onto Al_2O_3 or $MgAl_2O_4$ were the COP materials with the highest Cu content that also presented high chemical stability.

In Figure 6a the SEM images of fresh samples of the selected CuO-based materials in powder form are shown in a scale of 10 μm. The SEM analysis carried out to the selected samples with Cu loads around 65 %wt. in oxidized form showed that there is a homogeneous dispersion of CuO on to the inert support in both solids. The light areas of SEM images are related with the presence of Cu, and the dark grey zones indicate the presence of Al and/or Mg. It can be appreciated in the Figure that copper particles were a bit smaller than the particles of the material used as support. Regardless the support used, the $MgAl_2O_4$ material showed substantially smaller particles than the Al_2O_3. Finally, both materials presented a homogeneous dispersion of the compounds throughout all the sample.

3.2.2. Materials in pellet form

The materials selected in powder form as optimal candidates for the Ca/Cu looping process were pelletized in order to analyze their mechanical stability. In addition the Cu material with the highest Cu load (70 %wt.) onto $MgAl_2O_4$ was also pelletized to determine the limit of Cu load that can reach this type of materials. In this way three types of pellets (P_Cu65Al_COPa, P_Cu65Al_COPb, P_Cu65Al_COPc) were prepared

from the Cu65Al_COP powder, whose main difference was the pellet density. Small quantities of a material used as a binder was incorporated during the preparation of the pellets onto Al_2O_3, and therefore the Cu content in these pellets decreased a bit (Cu load around 60%wt.) with respect to the pellets supported on to $MgAl_2O_4$ (without binder material). In addition, pellets from the Cu65MgAl_COP and Cu70MgAl_COP materials were also prepared (P_Cu65MgAl_COP, P_Cu70MgAl_COP). Table 2 details the main characteristics of the pellets.

Table 2: Characteristics of pellets supported on Al_2O_3 and $MgAl_2O_4$ made from the selected powdered materials. *The dimensions of the pellets are: diameter = height = $3.3 \cdot 10^{-3}$ m for the pellets onto Al_2O_3 and diameter = height = $3.0 \cdot 10^{-3}$ m for the pellets onto $MgAl_2O_4$.*

Reference	Origin material	ρ (kg m^{-3})	%wt. Cu	ε (%)	OTC (mgO mg $solid^{-1}$)
P_Cu65Al_COP_a	Cu65Al_COP	2300	59.4	48	0.149
P_Cu65Al_COP_b	Cu65Al_COP	2900	57.5		0.143
P_Cu65Al_COP_c	Cu65Al_COP	2540	58.8	43	0.148
P_Cu70MgAl_COP	Cu70MgAl_COP	2160	69.0		0.174
P_Cu65MgAl_COP	Cu65MgAl_COP	2260	65.0		0.160

The materials were cut and the cross-section was analyzed by SEM-EDX to determine their homogeneity. Figure 6(b) shows an example of the SEM images, photographs and EDX figures obtained for the two different pellets produced with the different supports (P_Cu65Al_COP and P_Cu65MgAl_COP). The EDX applied to the pellets diameter showed an homogeneous dispersion of the Cu^{2+}, Al^{3+} and Mg^{2+} ions when present. In

the mapping obtained by EDX to the Cu and Al elements individually, can be appreciated a uniform distribution of the elements throughout both pellets.

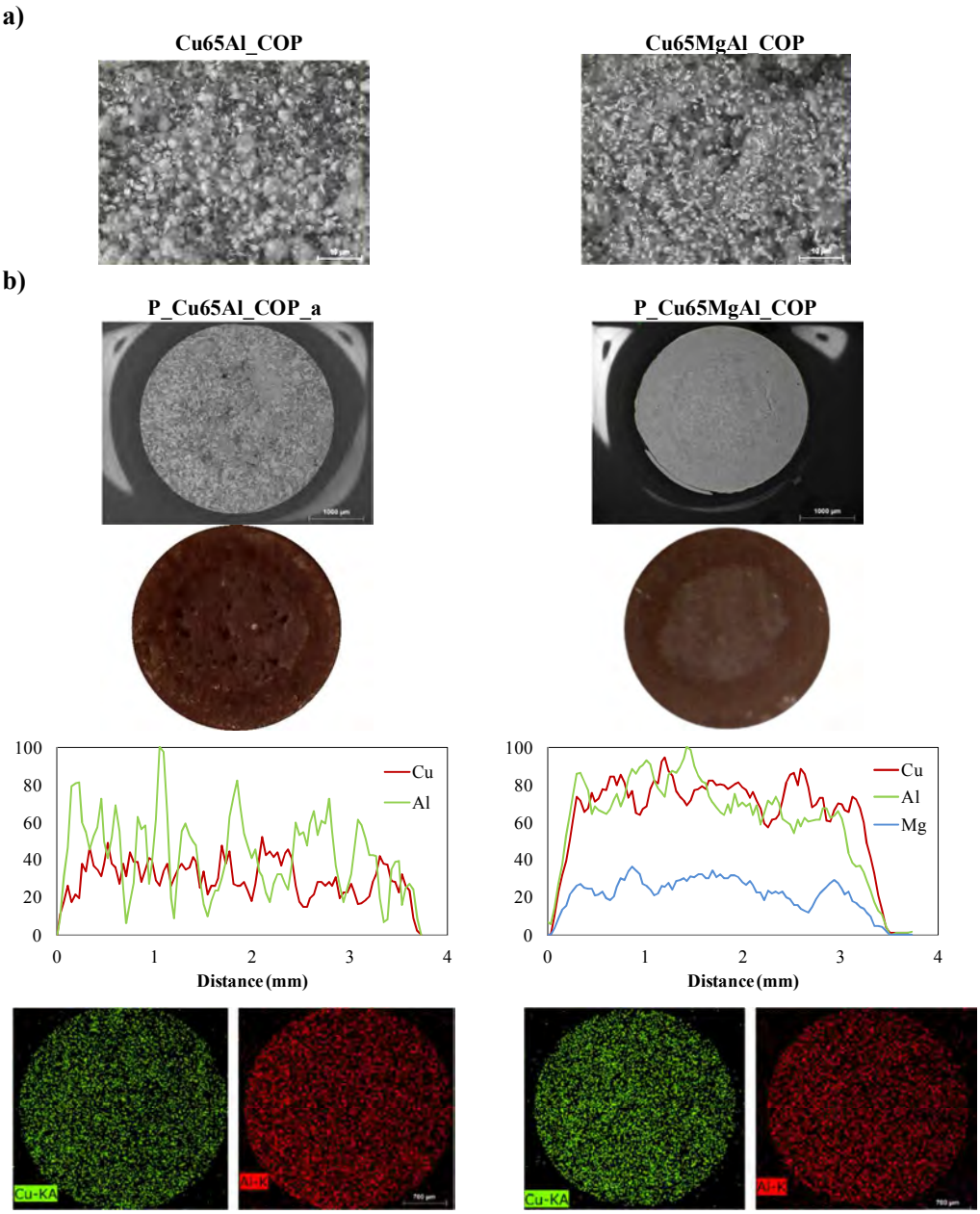

Figure 6: a) *SEM images for fresh selected materials in powder form;* ***b)*** *SEM and EDX analysis for fresh pellets: SEM images (first row), photographs (second row) and EDX figures (third row).*

Following a similar procedure as done for the materials in powder form the evolution of pellets oxygen transport capacity with the number of reaction cycles was assessed in the TGA apparatus described in the experimental section. Figure 7a (left) shows the evolution of OTC (mg O/mg oxidized material) during more than 150 reaction cycles of the COP materials with 65 %wt. of Cu load on to Al_2O_3 and $MgAl_2O_4$. According to the Figure, both materials presented highly stable oxygen transport capacity with maximum losses of 1% of OTC in the last cycles.

It must be highlighted that the materials in pellet form showed similar OTC values to the powders which means that all the Cu remains active during the oxidation and reduction reactions and there is no formation of inaccessible sites of copper inside the pellet along the cycles. In the case of the OTC of the pellet onto Al_2O_3, the value has been slightly reduced with respect to the pellet onto $MgAl_2O_4$ due to the addition of small quantities of binder as it has been mentioned in the previous paragraphs.

Regarding to the oxidation conversion curves of the pellets supported on Al_2O_3 synthesized by Johnson Matthey for cycles 50 and 100 (Figure 7 (a, right)), it can be observed that all the pellets reach complete conversion in less than 4 minutes but slight differences on the slope of the curves among the materials can be appreciated. These differences are more relevant during the 50^{th} cycle being the P_Cu65Al_COP_b which presents the smaller slope followed by P_Cu65Al_COP_c. In addition, these pellets that have the greatest values of density presented slightly slower reaction rates at the initial cycles which could be due to the decrease in porosity of these materials and therefore the slightly greater difficulty to the O_2 to access to the Cu active sites.

However it can be observed that the slope of the oxidation conversion of the three pellets is practically the same in the 100^{th} cycle which means that the oxygen is able to easily access inside the pellet as long as the cycles proceed. As well as the reduction

conversion curves of the materials in powder form, no remarkable differences were detected among materials in the reduction curves of the pellets as these curves were highly repetitive in terms of the number of cycles and the reduction occurred very fast.

In view of the results obtained for the chemical stability of the pellets with 65 %wt. onto Al_2O_3, a similar study was carried out for the pellet with 65 %wt. onto $MgAl_2O_4$. Besides, the mechanical stability of the material with 70 %wt. onto $MgAl_2O_4$ was tested. Figure 7 (b, left) shows the evolution of OTC (mg O/mg oxidized material) during more than 150 reaction cycles of the COP materials with 65 and 70 %wt. of Cu load onto $MgAl_2O_4$. According to this Figure, the OTC of the pellet with 65 %wt. of Cu load remained highly stable along 150 cycles. However, the loss in the OTC in the pellet with 70%wt. of Cu can be clearly appreciated and it descends slowly and progressively from cycle 1 to cycle 150. Then, there seems to be a limit in Cu content to obtain highly stable materials and this limit has been found around 70%wt of Cu load for the Al_2O_3 and $MgAl_2O_4$ supports. It seems that an increase up to 70%wt. of Cu load in the material results in a non-homogeneous mixture between the different phases present in the material. This aspect together with the decrease in hardness of the pellet due to the reduction of spinel content [87], which is required in a certain proportion since it allows the improvement of the mechanical properties of the pellet, makes that there is a maximum Cu load in the materials that should not be exceeded to develop highly stable materials.

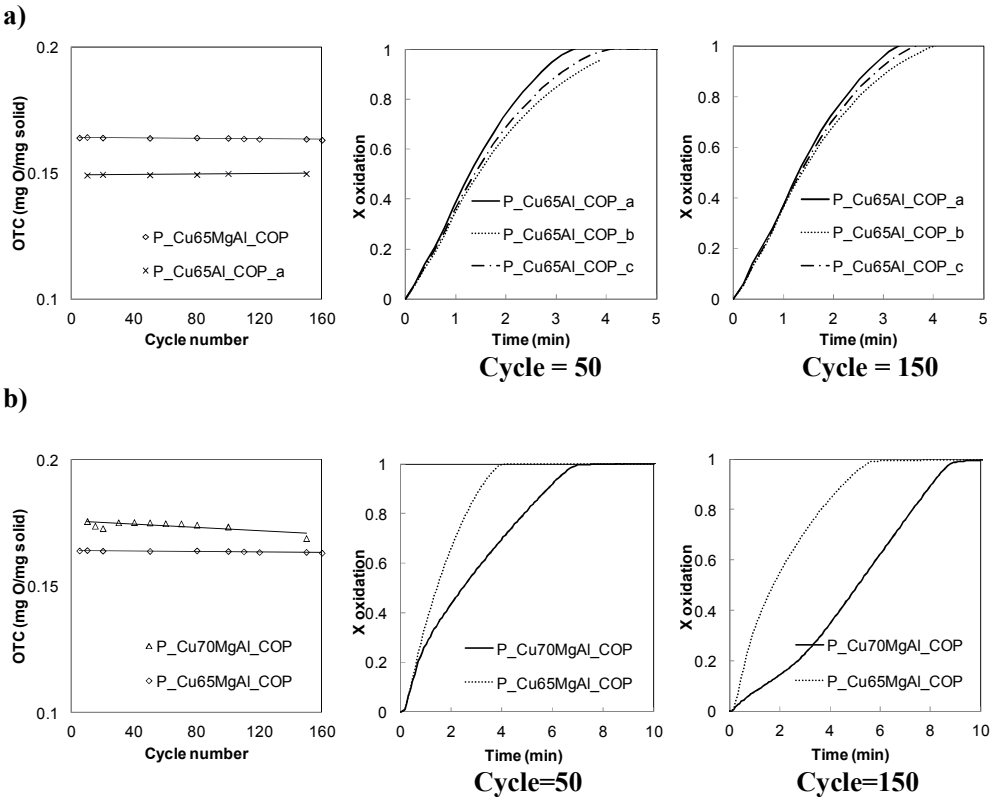

Figure 7: a) *Left: OTC for pellets with Cu load around 65%wt. on to Al_2O_3 and $MgAl_2O_4$ during approximately 150 oxidation-reduction cycles. Right: Oxidation curves for pellets with different characteristics made from the powdered material Cu65Al_COP with 20vol% O_2 at 870ºC (cycles = 50 and 100);* ***b)*** *Left: OTC for pellets on to $MgAl_2O_4$ with 65%wt. and 70%wt. during approximately 150 oxidation-reduction cycles. Right: Oxidation curves for CuO-Al_2O_3 and CuO-$MgAl_2O_4$ pellets with 20vol% O_2 at 870ºC: (left) cycle = 50, (right) cycle = 150.*

Finally, an additional study was carried out in order to analyze the mechanical strength of several pellets after cycles in oxidized and reduced conditions. Three pellets made from the powdered material synthesized by COP and supported on Al_2O_3 with 65wt% of Cu load, but with different physical properties (P_Cu65Al_COP_a, P_Cu65Al_COP_b and P_Cu65Al_COP_c), were tested in a Shimpo Dynamometer to determine the horizontal crushing strength after several number of cycles (10, 50, 75,

100, 200), both in oxidized and reduced forms. In Figure 8a the values of horizontal crushing strength (HCS) of oxidized and reduced pellets tested for different redox cycles are plotted.

The oxidized pellets followed a progressive trend of increase in strength during the first 35 - 45 cycles, achieving values of HCS up to 55 N in all cases. After this period, during the cycles 60 - 100 two pellets (P_CuAl_COP_b and P_CuAl_COP_c) lose strength until values around 60 N and other keep similar values during these cycles (P_CuAl_COP_a). In this way, the pellet P_Cu65Al_b, that is the material with the highest density, showed the highest increase on strength (until 80 N approximately) however the prompt drop in HCS was also produced in oxidized and reduced forms.

On the other hand, the reduced pellets were initially hardest than the oxidized and although the pellet with the greater density showed a rapid drop, the other pellets keeping similar values of HCS for 80 cycles.

Therefore the pellet with the lowest density (P_Cu65Al_COP_a) presented the best mechanical behavior in multiple cycles. The HCS values for both oxidized and reduced pellet of P_Cu65Al_COP_a after 175 cycles are reported in Figure 8b. As it can be concluded by this study, the pellet with the lowest density is associated also with the highest porosity value which would decrease the thermal shock resistance produced during cycles. It is also interesting to highlight that the HCS values of this pellet during the course of the cycles in oxidized and reduced forms were very similar which is a very important aspect in order to develop materials with high mechanical resistance to oxidizing and reducing conditions at high temperature.

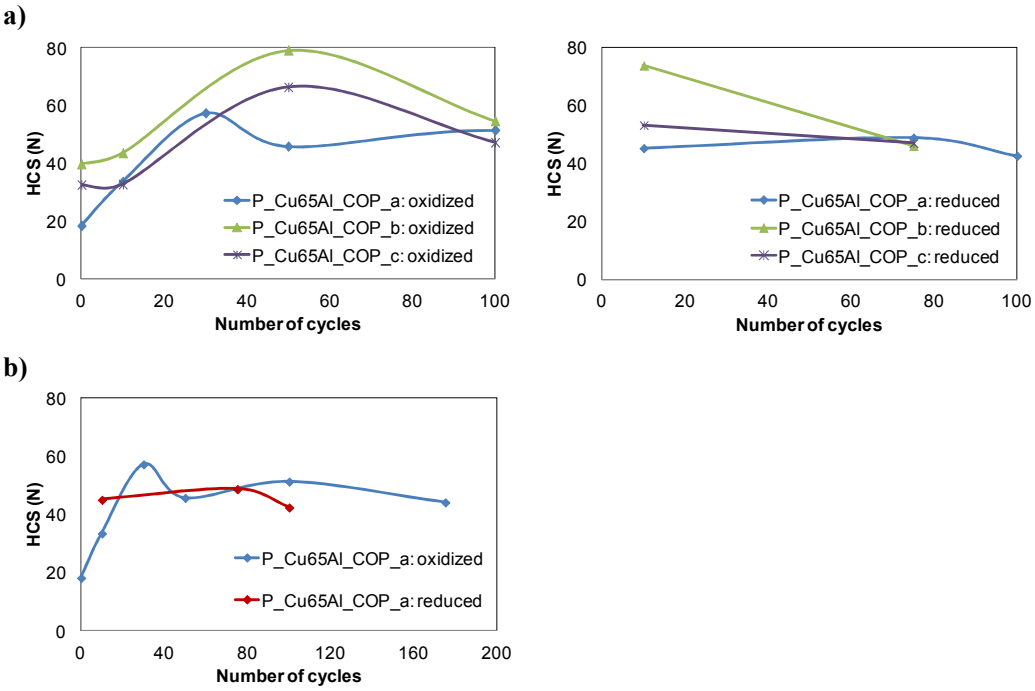

Figure 8: a) *Horizontal crushing strength in 100 cycles of oxidized pellets (left) and reduced pellets (right);* ***b)*** *Horizontal crushing strength in oxidized and reduced pellets of S0397-1047-2 along 175 cycles.*

4. CONCLUSIONS

Materials with Cu contents between 48 %wt. to 75 %wt. supported onto Al_2O_3, $MgAl_2O_4$ and ZrO_2 were synthesized by SP, COP, DEP and MM. Highly stable materials with Cu loads around 65%wt. onto Al_2O_3 and $MgAl_2O_4$ has been obtained by COP. The results confirmed a good dispersion between the active phase and the support in both, materials in powder and pellet form. It is essential not to exceed the amount of boundary copper that the material is capable of containing in order to obtain a good dispersion of the different phases inside the material as an increase until 70%wt. of Cu in pellets meant a marked decrease in oxidation reaction rate after cycles. On the other

hand, materials onto ZrO_2 with similar Cu content by COP showed a progressive lost in oxygen transport capacities from the first cycles which it has been associated to the formation of monoclinic ZrO_2. On the other hand, SD and DP were not a suitable routes for this kind of materials as materials by SD presented low specific surface areas and the DP method resulted in materials with very large CuO crystals.

The evolution of the OTC of the selected materials in powder form was fairly stable along 100 reduction/oxidation cycles. In the same way, the mechanical stability of the pellets during 150 cycles has been successfully confirmed and the oxygen transport capacity was evaluated finding a maximum loss of 1% in the last cycles. Similar HCS values and no agglomeration signs along multiple cycles were found for the pellets which is a very important result since the point of view of the mechanical stability and therefore these pellets are suitable candidates for the Ca/Cu process. Moreover, the scaling up of the co-precipitation procedure would not present too many difficulties because of the simplicity of the equipment and the good homogeneity obtained by this method.

Acknowledgements

This work acknowledges the support by European Union Seventh Frame Programme FP7 under grant agreement n° 608512 (ASCENT Project). Laura Díez acknowledges the FPI fellowship (ENE 2012-37936-CO2-01, BES-2013-064616 financed by MINECO).

REFERENCES

(1) IEA. Hydrogen and Fuel Cells, in: I. Publications (Ed.) Technology Roadmap, Paris, France, **2015**.

(2) Metz, B. D., O., de Coninck H.;, Loos, m.; Meyer, L., IPCC Special Report on Carbon Dioxide Capture and Storage. Prepared by Working Group III of the Intergovernmental Panel on Climate Change. *Cambridge University Press* **2005**, 442.

(3) IEA. CO2 emissions from fuel combustion, Paris, France, **2017**.

(4) J. Ruether, M. R., E. Grol :"Life-Cycle Analysis of Greenhouse Gas Emissions for Hydrogen Fuel Production in the United States from LNG and Coal". DOE/NETL-2006/1227. National Energy Technology Laboratory. **2005**.

(5) Damen, K.; Troost, M. v.; Faaij, A.; Turkenburg, W., A comparison of electricity and hydrogen production systems with CO2 capture and storage. Part A: Review and selection of promising conversion and capture technologies. *Prog. Energy Combust. Sci.* **2006,** *32*, 215-246.

(6) Kumar, A.; Edgar, T. F.; Baldea, M., Multi-resolution model of an industrial hydrogen plant for plantwide operational optimization with non-uniform steam-methane reformer temperature field. *Comput. Chem. Eng.* **2017**, *107*, 271-283.

(7) Abanades, J. C.; Murillo, R.; Fernandez, J. R.; Grasa, G.; Martínez, I., New CO2 Capture Process for Hydrogen Production Combining Ca and Cu Chemical Loops. *Environ. Sci. Technol.* **2010,** *44*, 6901-6904.

(8) Harrison, D. P., Sorption-Enhanced Hydrogen Production: A Review. *Ind. Eng. Chem. Res.* **2008,** *47*,6486-6501.

(9) Fernández, J. R.; Abanades, J. C.; Murillo, R.; Grasa, G., Conceptual design of a hydrogen production process from natural gas with CO2 capture using a Ca–Cu chemical loop. *Int. J. Greenhouse Gas Control* **2012,** *6*, 126-141.

(10) Weimer, T.; Berger, R.; Hawthorne, C.; Abanades, J. C., Lime enhanced gasification of solid fuels: Examination of a process for simultaneous hydrogen production and CO2 capture. *Fuel* **2008,** *87*, 1678-1686.

(11) Meyer, J.; Mastin, J.; Bjørnebøle, T.-K.; Ryberg, T.; Eldrup, N., Techno-economical study of the Zero Emission Gas power concept. *Energy Procedia* **2011,** *4*, 1949-1956.

(12) Junk, M.; Reitz, M.; Ströhle, J.; Epple, B., Thermodynamic Evaluation and Cold Flow Model Testing of an Indirectly Heated Carbonate Looping Process. *Chem. Eng. Technol.* **2013,** *36*, 1479-1487.

(13) Fernández, J. R.; Abanades, J. C., CO2 capture from the calcination of CaCO3 using iron oxide as heat carrier. *J. Cleaner Prod.* **2016,** *112*, 1211-1217.

(14) Rodríguez, N.; Alonso, M.; Grasa, G.; Abanades, J. C., Process for Capturing CO2 Arising from the Calcination of the CaCO3 Used in Cement Manufacture. *Environ. Sci. Technol.* **2008,** *42*, 6980-6984.

(15) Wolf, J.; Yan, J., Parametric study of chemical looping combustion for tri-generation of hydrogen, heat, and electrical power with CO2 capture. *Int. J. Energy Res.* **2005,** *29*, 739-753.

(16) Abanades, J. C.; Murillo, V. R., Method for recovering co2 by means of cao and the exothermic reduction of a solid. **2009**, (PCT/ES2010/070585).

(17) Boot-Handford, M. E.; Abanades, J. C.; Anthony, E. J.; Blunt, M. J.; Brandani, S.; Mac Dowell, N.; Fernandez, J. R.; Ferrari, M.-C.; Gross, R.; Hallett, J. P.; Haszeldine, R. S.; Heptonstall, P.; Lyngfelt, A.; Makuch, Z.; Mangano, E.; Porter, R. T. J.; Pourkashanian, M.; Rochelle, G. T.; Shah, N.; Yao, J. G.; Fennell, P. S., Carbon capture and storage update. *Energy Environ. Sci.* **2014,** *7*, 130-189.

(18) Rostrup-Nielsen, J. R.; Sehested, J.; Nørskov, J. K., Hydrogen and synthesis gas by steam- and C02 reforming. *Adv. Catal.* **2002**, *47*, 65-139.

(19) Meerman, J. C.; Hamborg, E. S.; van Keulen, T.; Ramírez, A.; Turkenburg, W. C.; Faaij, A. P. C., Techno-economic assessment of CO2 capture at steam methane reforming facilities using commercially available technology. *Int. J. Greenhouse Gas Control* **2012,** *9*, 160-171.
(20) Martínez, I.; Romano, M. C.; Chiesa, P.; Grasa, G.; Murillo, R., Hydrogen production through sorption enhanced steam reforming of natural gas: Thermodynamic plant assessment. *Int. J. Hydrogen Energy* **2013,** *38*, 15180-15199.
(21) Martínez, I.; Romano, M. C.; Fernández, J. R.; Chiesa, P.; Murillo, R.; Abanades, J. C., Process design of a hydrogen production plant from natural gas with CO2 capture based on a novel Ca/Cu chemical loop. *Appl. Energy* **2014,** *114*, 192-208.
(22) Fernández, J. R.; Alarcón, J. M.; Abanades, J. C., Investigation of a Fixed-Bed Reactor for the Calcination of CaCO3 by the Simultaneous Reduction of CuO with a Fuel Gas. *Ind. Eng. Chem. Res.* **2016,** *55*, 5128-5132.
(23) Fernandez, J. R.; Abanades, J. C.; Murillo, R., Modeling of sorption enhanced steam methane reforming in an adiabatic fixed bed reactor. *Chem. Eng. Sci.* **2012,** *84*, 1-11.
(24) Fernandez, J. R.; Abanades, J. C.; Grasa, G., Modeling of sorption enhanced steam methane reforming—Part II: Simulation within a novel Ca/Cu chemical loop process for hydrogen production. *Chem. Eng. Sci.* **2012,** *84*, 12-20.
(25) Fernandez, J. R.; Abanades, J. C.; Murillo, R., Modeling of Cu oxidation in an adiabatic fixed-bed reactor with N2 recycling. *Appl. Energy* **2014,** 113, 1945-1951.
(26) Martini, M.; van den Berg, A.; Gallucci, F.; van Sint Annaland, M., Investigation of the process operability windows for Ca-Cu looping for hydrogen production with CO2 capture. *Chem. Eng. J.* **2016,** *303*, 73-88.
(27) Fernández, J. R.; Abanades, J. C., Optimized design and operation strategy of a CaCu chemical looping process for hydrogen production. *Chem. Eng. Sci.* **2017,** *166*, 144-160.
(28) Grasa, G.; Navarro, M. V.; López, J. M.; Díez-Martín, L.; Fernández, J. R.; Murillo, R., Validation of the H2 production stage via SER under relevant conditions for the Ca/Cu reforming process practical application. *Chem. Eng. J.* **2017,** *324*, 266-278.
(29) Manovic, V.; Anthony, E. J., Integration of Calcium and Chemical Looping Combustion using Composite CaO/CuO-Based Materials. *Environ. Sci. Technol.* **2011,** *45*, 10750-10756.
(30) Manovic, V.; Wu, Y.; He, I.; Anthony, E. J., Core-in-Shell CaO/CuO-Based Composite for CO2 Capture. *Industrial & Engineering Chemistry Research* **2011,** *50*, 12384-12391.
(31) Rahman, R. A.; Mehrani, P.; Lu, D. Y.; Anthony, E. J.; Macchi, A., Investigating the Use of CaO/CuO Sorbents for in Situ CO2 Capture in a Biomass Gasifier. *Energy Fuels* **2015,** *29*, 3808-3819.
(32) Qin, C.; Yin, J.; Liu, W.; An, H.; Feng, B., Behavior of CaO/CuO Based Composite in a Combined Calcium and Copper Chemical Looping Process. *Ind. Eng. Chem. Res.* **2012,** *51*, 12274-12281.
(33) Kierzkowska, A. M.; Muller, C. R., Development of calcium-based, copper-functionalised CO2 sorbents to integrate chemical looping combustion into calcium looping. *Energy Environ. Sci.* **2012,** *5*, 6061-6065.
(34) Ridha, F. N.; Lu, D.; Macchi, A.; Hughes, R. W., Combined calcium looping and chemical looping combustion cycles with CaO–CuO pellets in a fixed bed reactor. *Fuel* **2015,** *153*, 202-209.
(35) Satrio, J. A.; Shanks, B. H.; Wheelock, T. D., Development of a Novel Combined Catalyst and Sorbent for Hydrocarbon Reforming. *Ind. Eng. Chem. Res.* **2005,** *44*, 3901-3911.
(36) Satrio, J. A.; Shanks, B. H.; Wheelock, T. D., A Combined Catalyst and Sorbent for Enhancing Hydrogen Production from Coal or Biomass. *Energy Fuels* **2007,** *21*, 322-326.
(37) Martavaltzi, C. S.; Lemonidou, A. A., Hydrogen production via sorption enhanced reforming of methane: Development of a novel hybrid material—reforming catalyst and CO2 sorbent. *Chem. Eng. Sci.* **2010,** *65*, 4134-4140.
(38) Chanburanasiri, N.; Ribeiro, A. M.; Rodrigues, A. E.; Arpornwichanop, A.; Laosiripojana, N.; Praserthdam, P.; Assabumrungrat, S., Hydrogen Production via Sorption Enhanced Steam

Methane Reforming Process Using Ni/CaO Multifunctional Catalyst. *Ind. Eng. Chem. Res.* **2011,** *50*, 13662-13671.
(39) García-Lario, A. L.; Grasa, G. S.; Murillo, R., Performance of a combined CaO-based sorbent and catalyst on H2 production, via sorption enhanced methane steam reforming. *Chem. Eng. J.* **2015,** *264*, 697-705.
(40) de Diego, L. F.; García-Labiano, F.; Adánez, J.; Gayán, P.; Abad, A.; Corbella, B. M.; María Palacios, J., Development of Cu-based oxygen carriers for chemical-looping combustion. *Fuel* **2004,** *83*, 1749-1757.
(41) de Diego, L. F.; García-Labiano, F.; Gayán, P.; Celaya, J.; Palacios, J. M.; Adánez, J., Operation of a 10 kWth chemical-looping combustor during 200 h with a CuO–Al2O3 oxygen carrier. *Fuel* **2007,** *86*, 036-1045.
(42) Gayán, P.; Forero, C. R.; Abad, A.; de Diego, L. F.; García-Labiano, F.; Adánez, J., Effect of support on the behavior of Cu-based oxygen carriers during long-term CLC operation at temperatures above 1073 K. *Energy Fuels* **2011,** *25*, 1316-1326.
(43) CaO, Y. C., Z.X.; Meng, L.; Riley, J.T.; Pan, W.P. , Reduction of solid oxygen carrier (CuO) by solid fuel (coal) in chemical looping combustion. *Prepr. Symp. - Am. Chem. Soc., Div. Fuel Chem.* **2005**, *50*, 99-102.

(44) Roux, S. B., A.; Antonini, G., Study and improvement of the regeneration of metallic oxides used as oxygen carriers for a new combustion process. *Int. J. Chem. React. Eng.* **2006,** *4*.
(45) Tian, H.; Chaudhari, K.; Simonyi, T.; Poston, J.; Liu, T.; Sanders, T.; Veser, G.; Siriwardane, R., Chemical-looping Combustion of Coal-derived Synthesis Gas Over Copper Oxide Oxygen Carriers. *Energy Fuels* **2008,** *22*, 3744-3755.
(46) Siriwardane, R.; Tian, H.; Richards, G.; Simonyi, T.; Poston, J., Chemical-Looping Combustion of Coal with Metal Oxide Oxygen Carriers. *Energy Fuels* **2009,** *23*, 3885-3892.
(47) Rubel, A.; Liu, K.; Neathery, J.; Taulbee, D., Oxygen carriers for chemical looping combustion of solid fuels. *Fuel* **2009,** *88*, 876-884.
(48) Abad, A.; Adánez, J.; García-Labiano, F.; de Diego, L. F.; Gayán, P., Modeling of the chemical-looping combustion of methane using a Cu-based oxygen-carrier. *Combust. Flame* **2010,** *157*, 602-615.
(49) Arjmand, M.; Azad, A.-M.; Leion, H.; Mattisson, T.; Lyngfelt, A., Evaluation of CuAl2O4 as an Oxygen Carrier in Chemical-Looping Combustion. *Ind. Eng. Chem. Res.* **2012,** *51*, 13924-13934.
(50) Imtiaz, Q.; Kierzkowska, A. M.; Müller, C. R., Coprecipitated, Copper-Based, Alumina-Stabilized Materials for Carbon Dioxide Capture by Chemical Looping Combustion. *ChemSusChem* **2012,** *5*, 1610-1618.
(51) Song, Q.; Liu, W.; Bohn, C. D.; Harper, R. N.; Sivaniah, E.; Scott, S. A.; Dennis, J. S., A high performance oxygen storage material for chemical looping processes with CO2 capture. *Energy Environ. Sci.* **2013,** *6*, 288-298.
(52) Imtiaz, Q.; Kurlov, A.; Rupp, J. L. M.; Müller, C. R., Highly Efficient Oxygen-Storage Material with Intrinsic Coke Resistance for Chemical Looping Combustion-Based CO2 Capture. *ChemSusChem* **2015,** *8*, 2055-2065.
(53) Gayán, P.; Adánez-Rubio, I.; Abad, A.; de Diego, L. F.; García-Labiano, F.; Adánez, J., Development of Cu-based oxygen carriers for Chemical-Looping with Oxygen Uncoupling (CLOU) process. *Fuel* **2012,** *96*, 226-238.
(54) Rydén, M.; Jing, D.; Källén, M.; Leion, H.; Lyngfelt, A.; Mattisson, T., CuO-Based Oxygen-Carrier Particles for Chemical-Looping with Oxygen Uncoupling – Experiments in Batch Reactor and in Continuous Operation. *Ind. Eng. Chem. Res.* **2014,** *53*, 6255-6267.
(55) Adánez-Rubio, I.; Gayán, P.; García-Labiano, F.; de Diego, L. F.; Adánez, J.; Abad, A., Development of CuO-based oxygen-carrier materials suitable for Chemical-Looping with Oxygen Uncoupling (CLOU) process. *Energy Procedia* **2011,** *4*, 417-424.

(56) Mattisson, T.; Lyngfelt, A.; Leion, H., Chemical-looping with oxygen uncoupling for combustion of solid fuels. *Int. J. Greenhouse Gas Control* **2009,** *3*, 11-19.
(57) Adánez-Rubio, I. G., P.; Abad, A.; García-Labiano, F.; de Diego, L.F.; Adánez, J., CO2 capture in coal combustion by chemical-looping with oxygen uncoupling (CLOU) with a Cu-based oxygen carrier. *5º International Conference on Clean Coal Technologies (CCT2011). Zaragoza, Spain.* **2011**.
(58) Imtiaz, Q.; Broda, M.; Müller, C. R., Structure–property relationship of co-precipitated Cu-rich, Al2O3- or MgAl2O4-stabilized oxygen carriers for chemical looping with oxygen uncoupling (CLOU). *Appl. Energy* **2014,** *119*, 557-565.
(59) Arjmand, M.; Leion, H.; Mattisson, T.; Lyngfelt, A., ZrO2-Supported CuO Oxygen Carriers for Chemical-Looping with Oxygen Uncoupling (CLOU). *Energy Procedia* **2013,** *37*, 550-559.
(60) Zafar, Q.; Mattisson, T.; Gevert, B., Redox Investigation of Some Oxides of Transition-State Metals Ni, Cu, Fe, and Mn Supported on SiO2 and MgAl2O4. *Energy Fuels* **2006,** *20*, 34-44.
(61) Zafar, Q.; Mattisson, T.; Gevert, B., Integrated Hydrogen and Power Production with CO2 Capture Using Chemical-Looping ReformingRedox Reactivity of Particles of CuO, Mn2O3, NiO, and Fe2O3 Using SiO2 as a Support. *Ind. Eng. Chem. Res.* **2005,** *44*, 3485-3496.
(62) García-Lario, A. L.; Martínez, I.; Murillo, R.; Grasa, G.; Fernández, J. R.; Abanades, J. C., Reduction Kinetics of a High Load Cu-based Pellet Suitable for Ca/Cu Chemical Loops. *Ind. Eng. Chem. Res.* **2013,** *52*, 1481-1490.
(63) Lyngfelt, A.; Linderholm, C., Chemical-Looping Combustion of Solid Fuels – Status and Recent Progress. *Energy Procedia* **2017,** *114*, 371-386.
(64) Adánez, J.; de Diego, L. F.; García-Labiano, F.; Gayán, P.; Abad, A.; Palacios, J. M., Selection of Oxygen Carriers for Chemical-Looping Combustion. *Energy Fuels* **2004,** *18*, 371-377.
(65) Adanez, J.; Abad, A.; Garcia-Labiano, F.; Gayan, P.; de Diego, L. F., Progress in Chemical-Looping Combustion and Reforming technologies. *Prog. Energy Combust. Sci.* **2012,** *38*, 215-282.
(66) Arjmand, M.; Azad, A.-M.; Leion, H.; Lyngfelt, A.; Mattisson, T., Prospects of Al2O3 and MgAl2O4-Supported CuO Oxygen Carriers in Chemical-Looping Combustion (CLC) and Chemical-Looping with Oxygen Uncoupling (CLOU). *Energy Fuels* **2011,** *25*, 5493-5502.
(67) Chuang, S. Y.; Dennis, J. S.; Hayhurst, A. N.; Scott, S. A., Development and performance of Cu-based oxygen carriers for chemical-looping combustion. *Combust. Flame* **2008,** *154*, 109-121.
(68) Imtiaz, Q.; Kierzkowska, A. M.; Broda, M.; Müller, C. R., Synthesis of Cu-Rich, Al2O3-Stabilized Oxygen Carriers Using a Coprecipitation Technique: Redox and Carbon Formation Characteristics. *Environ. Sci. Technol.* **2012,** *46*, 3561-3566.
(69) Hu, W.; Donat, F.; Scott, S. A.; Dennis, J. S., The interaction between CuO and Al2O3 and the reactivity of copper aluminates below 1000 ºC and their implication on the use of the Cu-Al-O system for oxygen storage and production. *RSC Adv.* **2016,** *6*, 113016-113024.
(70) Arjmand, M.; Leion, H.; Mattisson, T.; Lyngfelt, A., ZrO2-Supported CuO Oxygen Carriers for Chemical-Looping with Oxygen Uncoupling (CLOU). *Energy Procedia* **2013,** *37*, 550-559.
(71) Hedayati, A.; Azad, A.-M.; Rydén, M.; Leion, H.; Mattisson, T., Evaluation of Novel Ceria-Supported Metal Oxides As Oxygen Carriers for Chemical-Looping Combustion. *Ind. Eng. Chem. Res.* **2012,** *51*, 12796-12806.
(72) Gombac, V.; Sordelli, L.; Montini, T.; Delgado, J. J.; Adamski, A.; Adami, G.; Cargnello, M.; Bernal, S.; Fornasiero, P., CuOx−TiO2 Photocatalysts for H2 Production from Ethanol and Glycerol Solutions. *J. Phys. Chem. A* **2010,** *114*, 3916-3925.
(73) Rydén, M.; Lyngfelt, A.; Mattisson, T.; Chen, D.; Holmen, A.; Bjørgum, E., Novel oxygen-carrier materials for chemical-looping combustion and chemical-looping reforming;

LaxSr1−xFeyCo1−yO3−δ perovskites and mixed-metal oxides of NiO, Fe2O3 and Mn3O4. *Int. J. Greenhouse Gas Control* **2008,** *2*, 21-36.

(74) Hu, C.-Y.; Shih, K.; Leckie, J. O., Formation of copper aluminate spinel and cuprous aluminate delafossite to thermally stabilize simulated copper-laden sludge. *J. Hazard. Mater.* **2010,** *181*, 399-404.

(75) Jacob, K.; B. Alcock, C., Thermodynamics of CuAlO2 and CuAl2O4 and Phase Equilibria in the System Copper(I) Oxide-Copper(II) Oxide-Aluminum Oxide. *J. Am. Ceram. Soc.* **2006,** *58*, 192-195.

(76) McCullough, J. D.; Trueblood, K. N., The crystal structure of baddeleyite (monoclinic ZrO2). *Acta Crystallogr.* **1959,** *12*, 507-511.

(77) Chevalier, J.; Gremillard, L.; Virkar, A. V.; Clarke, D. R., The Tetragonal-Monoclinic Transformation in Zirconia: Lessons Learned and Future Trends. *J. Am. Ceram. Soc.* **2009,** *92*, 1901-1920.

(78) Zhao, Y.; Tao, K.; Lin Wan, H., Effect of zirconia phase on the reduction behaviour of highly dispersed zirconia-supported copper oxide. *Catal.Commun.* **2004,** *5*, 249-252.

(79) Platt, P.; Frankel, P.; Gass, M.; Howells, R.; Preuss, M., Finite element analysis of the tetragonal to monoclinic phase transformation during oxidation of zirconium alloys. *J. Nucl. Mater.* **2014,** *454*, 290-297.

(80) Liu, Z.; Amiridis, M. D.; Chen, Y., Characterization of CuO Supported on Tetragonal ZrO2 Catalysts for N2O Decomposition to N2. *J. Phys. Chem.B* **2005,** *109*, 1251-1255.

(81) Águila, G.; Gracia, F.; Cortés, J.; Araya, P., Effect of copper species and the presence of reaction products on the activity of methane oxidation on supported CuO catalysts. *Appl. Catal., B* **2008,** *77*, 325-338.

(82) Ma, T.-Y.; Yuan, Z.-Y., Gold and CuO nanocatalysts supported on hierarchical structured Ce-doped titanias for low temperature CO oxidation. *Stud. Surf. Sci. Catal.* **2010**, *175*, 575-579.

(83) Liu, Y.; Guo, L.; Zhao, D.; Li, X.; Gao, Z.; Ding, T.; Tian, Y.; Jiang, Z., Enhanced activity of CuO/K2CO3/MgAl2O4 catalyst for lean NOx storage and reduction at high temperatures. *RSC Adv.* **2017,** *7*, 27405-27414.

(84) Yao, C.-Z.; Wang, L.-C.; Liu, Y.-M.; Wu, G.-S.; Cao, Y.; Dai, W.-L.; He, H.-Y.; Fan, K.-N., Effect of preparation method on the hydrogen production from methanol steam reforming over binary Cu/ZrO2 catalysts. *Appl. CataL., A* **2006,** *297*, 151-158.

(85) Pakharukova, V. P.; Moroz, E. M.; Zyuzin, D. A.; Ishchenko, A. V.; Dolgikh, L. Y.; Strizhak, P. E., Structure of Copper Oxide Species Supported on Monoclinic Zirconia. *J. Phys. Chem. C* **2015,** *119*, 28828-28835.

(86) Wang, Y.; Caruso, R. A., Preparation and characterization of CuO-ZrO2 nanopowders. *J. Mater. Chem.* **2002,** *12*, 1442-1445.

(87) Ganesh, I., A review on magnesium aluminate (MgAl2O4) spinel: synthesis, processing and applications. *Int. Mater. Rev.,* **2013,** *58*, 63-112.

Highly loaded $CuO\text{-}Al_2O_3$ pellet with long-term chemical and mechanical stability